Novel types of quantum criticality in heavy-fermion systems

Philipp Gegenwart, Frank Steglich, Christoph Geibel, M. Brando

Angaben zur Veröffentlichung / Publication details:

Gegenwart, Philipp, Frank Steglich, Christoph Geibel, and M. Brando. 2015. "Novel types of quantum criticality in heavy-fermion systems." *The European Physical Journal Special Topics* 224 (6): 975–96. https://doi.org/10.1140/epjst/e2015-02442-7.

Novel types of quantum criticality in heavy-fermion systems

P. Gegenwart[1,a], F. Steglich[2], C. Geibel[2], and M. Brando[2]

[1] Experimentalphysik VI, Center for Electronic Correlations and Magnetism, Augsburg University, 86159 Augsburg, Germany
[2] Max-Planck-Institut für Chemische Physik Fester Stoffe, Nöthnitzer Str. 40, 01187 Dresden, Germany

Abstract. Quantum criticality arises from continuous changes of matter at absolute zero temperature. It can have vast reaching influence on wide regions of phase space and is often connected to the occurrence of non-Fermi liquid behavior and unconventional superconductivity. Various different types of quantum criticality have been observed over the last years and $4f$-electron based heavy-fermion metals have become prototype materials in which quantum criticality is easily realized by application of pressure or magnetic field, as well as suitable changes in chemical composition. Using low-temperature thermodynamic, magnetic and transport experiments on clean prototype materials we investigate novel types of quantum criticality arising from ferromagnetic fluctuations and strong geometrical frustration, as well as quantum criticality hidden by unconventional superconductivity.

1 Introduction

Quantum critical points (QCPs) are of extensive current interest in condensed-matter physics as they can give rise to exotic finite-temperature properties. In addition, they promote the formation of novel phases, notably unconventional superconductivity or spin liquids. Heavy-fermion (HF) compounds have emerged as prototypical materials to study quantum criticality. A QCP occurs at the critical value of a non-thermal control parameter, e.g., pressure p, chemical substitution or magnetic field B, at which two ground states compete only at temperature $T = 0$. In metals the magnetic order can be of the spin-density-wave (SDW) type and the same electrons which form the Fermi surface are involved in the quantum phase transition (QPT). This is the case of HF compounds where the QPT separates a paramagnetic (PM) heavy Fermi liquid (FL) from an antiferromagnetic (AFM) metal [1–3]. In these systems there are two principal energy scales: $k_{\mathrm{B}}T_K$ and $k_{\mathrm{B}}T_{\mathrm{RKKY}}$ which derive from the respective interactions, the on-site Kondo and the inter-site RKKY interactions [4]. T_{K} defines the temperature at which the localized f-electrons start to hybridize with the itinerant d-electrons to, eventually, form a larger and heavier Fermi surface, T_{RKKY} is

[a] e-mail: gegenwph@physik.uni-augsburg.de

a measure of the inter-site exchange magnetic coupling. The interplay between these energy scales determines the magnetic ordering temperature T_N and characterizes the QPT [4]. In real systems, however, the situation can be rather more complex, due to the presence of multiple energy scales that can get involved in the QPT [5]: Spin, charge, orbital and lattice degrees of freedom have to be considered. In addition, several materials are prone to frustration and do not show any magnetic ordering but a spin liquid ground state. Others show more than just a single magnetic phase transition. In this respect, experimental studies on new quantum critical materials are desired. This is also a promising tool to discover novel correlated phases of condensed matter.

Theoretically, QCPs in HF metals have mostly been treated by applying the theory of order parameter fluctuations [6–8]. In this "conventional" approach it is assumed that the heavy, "composite" charge carriers keep their integrity at the QCP, i.e., they exist on either side of it. A prototype example is $CeCu_2Si_2$ [9,10]. This implies the AFM order to be of itinerant SDW type. The observation, through inelastic neutron scattering (INS), that the AFM correlations in the quantum critical material $CeCu_{5.9}Au_{0.1}$ are of a local character [11] has prompted theoretical descriptions of the QCP which include the destruction of the Kondo effect, respectively the disintegration of the composite fermions [12–16]. It has been pointed out, that a spin-liquid formation among the local moments, proposed e.g. for the presence of strong quantum fluctuations due to geometrical frustration, may act as competing mechanism against the Kondo-singlet formation [14,17,18], supporting novel types of quantum phase transitions. For example, continuous phase transitions associated with the onset of antiferromagnetism and deconfinement/topological order are possible or a so-called fractionalized Fermi liquid, which is induced by frustration and/or strong quantum fluctuations, where the f-moments decouple from the conduction electrons and have local character since there is no Kondo screening. Here, long-range magnetic order is precluded and the f-moments form an exotic metallic spin-liquid. The transition from a Fermi liquid with Kondo screening to fractionalized Fermi liquid, is the Kondo-breakdown transition (considered also as Mott transition of the f-electron subsystem) at which the Fermi volume changes. So far the relation between experimental control parameters, like pressure or magnetic field, and the strengths of frustration and T_K/J (with J the Heisenberg exchange constant) is unclear. Furthermore, the influence of disorder which often is introduced by chemical doping on these parameters must be investigated.

Although there is clear evidence for AFM QCPs [19,20], the existence of a ferromagnetic (FM) QCP is still open. In recent years, substantial experimental and theoretical efforts were made to investigate in detail this problem. However, it turned out that there are a wide range of possibilities. On theoretical grounds, a 3-dimensional (3D) itinerant (d-electron derived) FM QCP is believed to be inherently unstable, either towards a first-order phase transition or towards an inhomogeneous magnetic phase (modulated/textured structures) [21–24]. This behavior seems to be universal, i.e. valid for ferrimagnets as well as canted antiferromagnets provided the system is 2D or 3D [25]. Indeed several clean (stoichiometric) magnetic transition-metal compounds show non-Fermi liquid (NFL) behavior close to the FM instability, but the transition changes to first order (see, e.g., MnSi [26,27] or $ZrZn_2$ [28]). In other systems the existence of a FM QCP has been proposed, for instance in $Nb_{1-y}Fe_{2+y}$ [29] or $Zr_{1-x}Nb_xZn_2$ [30] where the FM-QCP is obtained by chemical substitution. However, in these cases the influence of disorder remains unsettled. More appropriate candidates are HF systems based on Yb or Ce elements [1,2], owing to their localized $4f$ shells. Unfortunately, the number of Yb-based systems close to a FM QCP is very limited. From the theoretical side it has been shown that a breakdown of the Kondo effect, i.e., a jump of the Fermi surface, can occur at $T = 0$ deeply inside

the ferromagnetically ordered state [31]. $YbNi_4P_2$ [32] and $YbCu_2Si_2$ [33] are rare examples of FM Kondo lattices, although $YbNi_4P_2$ has a quasi-1D crystalline and electronic structure which precludes this system to be understood within the approach valid for 2D or 3D systems (see [25,34] and next section). There are Ce-based alloys (e.g., $CePd_{1-x}Rh_x$ [35]), but here local disorder-driven mechanisms such as Kondo disorder or the quantum Griffiths phase scenario are responsible for the NFL properties [36–38]. Nevertheless, as it will be shown below, FM quantum critical phenomena are found in CeFePO and $YbNi_4P_2$.

For studying quantum criticality by thermodynamic means, Grüneisen parameters are important properties. The nature of pressure induced quantum criticality is thermodynamically best characterized by analyzing the divergence of the critical thermal Grüneisen ratio

$$\Gamma = \frac{\alpha}{C_p} = -\frac{(\partial S/\partial p)_T}{V_m T(\partial S/\partial T)_p} \tag{1}$$

where α is the volume thermal expansion coefficient and C_p the molar specific heat (after subtraction of non-critical contributions) [39,40]. Here, S is the entropy, V_m the molar volume and p the pressure. For a pressure-tuned quantum phase transition, the control parameter r can be linearized around the critical pressure $r = (p - p_c)/p_c$. The ratio $(\partial S/\partial p)_T = p_c^{-1}(\partial S/\partial r)_T$ explores then the dependence of the entropy on r. The corresponding quantity for a transition tuned by a magnetic field $H = B/\mu_0$ with $r = (H - H_c)/H_c$ is the critical magnetic Grüneisen parameter

$$\Gamma_H = -\frac{(\partial M/\partial T)_H}{C_H} = -\frac{1}{T}\frac{(\partial S/\partial H)_T}{(\partial S/\partial T)_H} = \frac{1}{T}\frac{\partial T}{\partial H}\Big|_S \tag{2}$$

where M is the total magnetization and C_H the specific heat at constant H. Γ_H can be thus measured directly by magnetocaloric effect experiments [41]. Scaling predicts $\Gamma \sim T^{-1/\nu z}$, with the correlation-length exponent ν and dynamical-critical exponent z. Whereas for an itinerant AFM QCP $\nu = 1/2$ and $z = 2$, resulting in $\Gamma \sim T^{-1}$, different exponents have been proposed for Kondo-breakdown QCPs [12,42].

In this paper, we review new results on ferromagnetic quantum criticality in the two Kondo lattice materials CeFePO (Sect. 2.1) and $YbNi_4P_2$ (Sect. 2.2). Furthermore, we focus on the geometrically frustrated Kondo lattice YbAgGe (Sect. 3.1) and the pyrochlore quantum spin ice $Pr_2Ir_2O_7$ (Sect. 3.2). In Sect. 4 we review recent results on quantum criticality hidden by superconductivity in $CeCoIn_5$; the paper ends with a summary in Sect. 5.

2 Ferromagnetic quantum criticality

In this section we present two newly discovered examples of HF systems which are close to a ferromagnetic instability, namely CeFePO and $YbNi_4P_2$. In both systems FM quantum fluctuations are very strong at low T, nevertheless their behavior at the FM quantum phase transition is very different: In CeFePO a short-range ordered state takes over at low-T although this is a stoichiometric system, and therefore no FM QCP is observed [43]. In $YbNi_4P_2$ evidence of a FM QCP was found by means of a measurement of the thermal Grüneisen ratio with no signature of a first order phase transition [34].

2.1 CeFePO

The layered Kondo-lattice system CeFePO is a unique candidate for studying FM-QCPs, because it is a clean non-magnetic HF metal located very close to a FM QCP

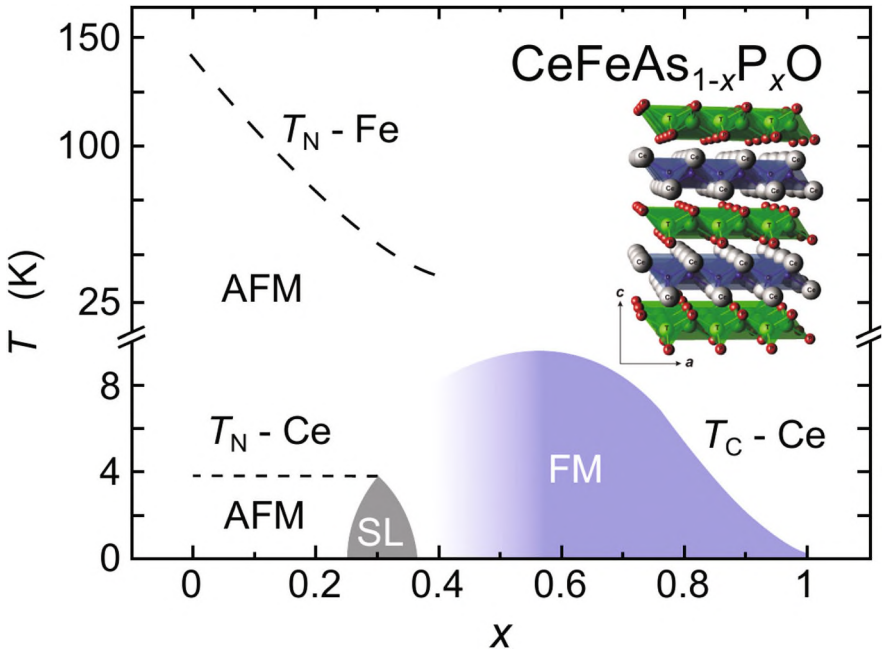

Fig. 1. Phase diagram of $CeFeAs_{1-x}P_xO$ adapted from Refs. [47,48]. This phase diagram was obtained from several measurement techniques on single and polycrystalline samples. The upper dashed line indicates the phase transition temperature T_N-Fe of the iron AFM ordering. The lower dashed line marks the AFM ordering of the Ce atoms. At $x \approx 0.3$ superconductivity was found within a small dome. The blue area corresponds to the FM ordered state only of the Ce atoms. At $x > 0.8$ the phase boundary line shows a tail similar to that found in the phase diagram of $CePd_{1-x}Rh_x$ [35]. The inset shows the ZrCuSiAs-type crystal structure ($P4/nmm$) of the CeTPO series with T = Ru, Os, Fe or Co [52].

with strong FM fluctuations [44,45]. CeFePO is a homologue of the quaternary iron pnictides RFeAsO (R = rare earth). Substituting As at the P site (As is larger than P) has the same effect as to apply negative pressure. Here, it introduces a volume effect by increasing mostly the c-axis. Negative pressure usually favors magnetic ordering in Ce-based systems. In fact, the ground state of the system $CeFeAs_{1-x}P_xO$ evolves from a long-range ordered FM ground state, when a small amount of arsenic is substituted for phosphorus. Less As concentration leads to a continuous decrease of T_C ending in a putative FM QCP. This was shown first by Luo et al. on polycrystals [46] and subsequently by Jesche et al. in single crystals [47,48]. The complete phase diagram of $CeFeAs_{1-x}P_xO$ is shown in Fig. 1. In CeFeAsO there is a commensurate AFM ordering of the Fe sublattice below $T \approx 140$ K which is suppressed by P substitution ending at a QCP at $x \approx 0.4$ [49]. Moreover, the Ce sublattice orders antiferromagnetically at 4.16 K. At $x \approx 0.4$ the Ce sublattice changes the ground state into a FM ordered state and keeps this state up to a P content of about 0.9. At $x = 1$ the system is a HF paramagnet with strong FM fluctuations, in agreement with Ref. [44]. In a small region close to $x = 0.3$ Jesche et al. found superconductivity which seems to coexist with Ce ferromagnetism [48]. However, experiments under hydrostatic pressure on single crystals of $CeFeAs_{1-x}P_xO$ revealed a much more complex interplay between superconductivity, Fe and Ce magnetism [50].

The isovalent P substitution not only reduces the volume but also increases locally the hybridization strength between the trivalent Ce-4f and the Fe-3D

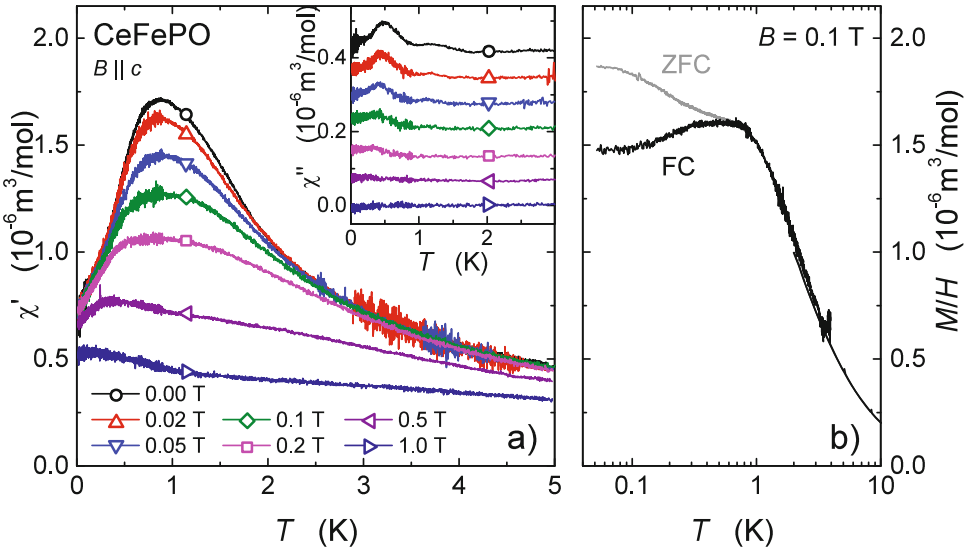

Fig. 2. AC-susceptibility $\chi'(T)$ of a single crystal of CeFePO measured with $B \parallel c$. Its imaginary part $\chi''(T)$ is shown in the inset. b) Zero-field-cooled and field-cooled magnetization measurements obtained at at $B = 0.1\,\mathrm{T}$ for the same crystal [43,56].

conduction electrons leading to an enhancement of the Kondo temperature $T_\mathrm{K} \approx 10\,\mathrm{K}$ for CeFePO [51]. Increasing x, the unit cell shrinks a factor of 3 more along the c-axis than along the a-axis indicating that the $f-d$ hybridization strength is controlled by the distance between the layers of OCe_4 tetrahedrons (cf. Fig. 1). In CeFePO, below T_K, the susceptibility and the Knight shift become field dependent and the NMR line width broadens. This identifies the onset of short-range FM correlations essentially within the basal plane, evidencing a strong anisotropy [44], which could also be confirmed by recent NMR measurements on oriented powder [53]. While approaching $x = 1$, the Curie temperature decreases not linearly with x but develops a tail, a signature of a smeared phase transition often observed in disordered ferromagnets like $CePd_{1-x}Rh_x$ [35]. However, in a recent and more detailed study C. Krellner and A. Jesche show that the ground state for $x = 0.9$ is AFM [47,54]. Therefore, it seems that $CeFeAs_{1-x}P_xO$ belongs to the systems which change their ordered state from FM to AFM when approaching the putative FM QCP, like, e.g., NbFe2 [55]. This suggests that a strong frustration has to be present in CeFePO as a result of competing interactions.

Frustration might be a crucial component to explain why we discovered a spin glass like ground state in poly and single crystalline CeFePO, since this is a stoichiometric compound where disorder should play a minor role [43]. A comprehensive study of the AC-susceptibility (χ'), specific heat (C) and muon-spin relaxation (μSR) measurements on high-quality single crystals is presented in Ref. [43]. We found evidence of strongly inhomogeneous spin fluctuations starting below T_K and of a short-range ordered state below $T_g \approx 0.9\,\mathrm{K}$ which prevents the system from accessing the putative FM QCP. We show in Fig. 2, as an example, a measurement of $\chi'(T)$ in a single crystal of CeFePO with magnetic field B applied along the c-axis and a measure of the zero-field-cooled (ZFC) and field-cooled (FC) magnetization at $B = 0.1\,\mathrm{T}$. The first evidence of spin freezing is seen in the T dependence of $\chi'(T)$ as a distinct peak at about T_g (Fig. 2a). At the peak, the susceptibility reaches values as high as $1.8 \cdot 10^{-6}\,\mathrm{m}^3/\mathrm{mol}$. The susceptibility is very anisotropic ($\chi_{\perp c}/\chi_{\parallel c} \approx 5$), and

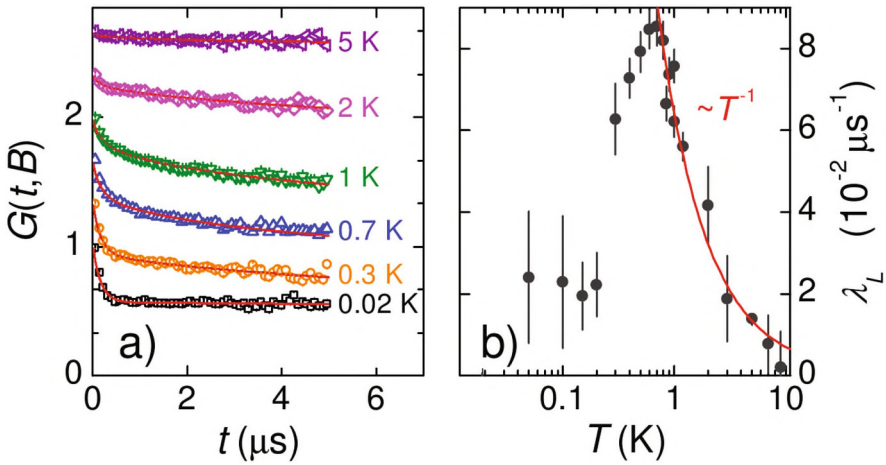

Fig. 3. a) Normalized muon-spin asymmetry function $G(t, B)$ at $B = 0.01\,\mathrm{T}$ for selected temperatures above and below T_g. Solid red lines are fits according to Eq. (3). The different curves are shifted by 0.33 for clarity. b) T-dependence of the dynamic μSR rate λ_L. The peak in $\lambda_L(T)$ undoubtly marks the magnetic transition from dynamic to static magnetism at $T_g \approx 0.8\,\mathrm{K}$. Figure extracted from Ref. [43].

with $B \perp c$ it reaches a high peak value of $9 \cdot 10^{-6}\,\mathrm{m}^3/\mathrm{mol}$. With increasing field its amplitude decreases and T_g shifts slightly. This observation confirms the presence of anisotropic FM spin fluctuations, that are much stronger in the basal plane. Dissipative effects are indicated by a peak in $\chi''(T)$ at about 0.5 K (inset of Fig. 2a), which is a significantly lower temperature than that of the maximum in $\chi'(T)$. A further indication of a spin glass like freezing is provided by the magnetization measurement in Fig. 2b. The ZFC and FC data split exactly at T_g, a standard signature of a spin glass state [57].

We have performed frequency dependent measurements of $\chi'(T)$ to investigate the magnetic ordering and spin dynamics. Similar to spin glasses, the maximum in $\chi'(T)$ shifts to higher temperatures as the excitation frequency is increased, while its amplitude decreases [43,56]. However, the dependence of T_g on the frequency is different from that found for canonical spin glasses [57]. A qualitatively similar behavior was found for $CePd_{1-x}Rh_x$ where the quantum Griffiths scenario was considered to explain the non-Fermi liquid thermodynamic properties and the evolution of $T_C(x)$ [35]. But, in CeFePO the magnetic anisotropy and the lack of evidence for FM cluster formation rule out such a mechanism. Moreover, we could not fit our data with $\chi \propto C/T \propto T^{\lambda-1}$ with $0 \leq \lambda \leq 1$ in any reasonable T-range as expected for this scenario [37]. The specific heat confirmed the bulk nature of the freezing by showing a broad maximum at about 0.55 K in a C/T vs. T plot. While at 0.1 T the maximum is unchanged, larger fields suppress it. Interestigly, the entropy connected with this maximum is surprisingly small, about 1% of $R\ln(2)$ in contrast to conventional spin glasses [57].

The microscopic nature of the low-T magnetism was studied by μSR measurements in zero and small longitudinal fields on a polycrystalline sample [43]. Figure 3a shows the T-evolution of the normalized muon-spin asymmetry function $G(t, B)$ at a constant field of $B = 0.01\,\mathrm{T}$ which is sufficient to quench the weak static relaxation due to nuclear dipole fields at the muon sites, leaving only the dynamic and static contributions due to the electronic Ce-4f magnetic moments. A quantitative analysis can be performed by considering the static and dynamical fields: The static relaxation

dominates $G(t, B)$ at short times t, while at long t the relaxation rate probes only the dynamic spin fluctuations. The used fitting function is

$$G(t, B) = G_1 \exp[-(\lambda_T t)] + G_2 \exp[-(\lambda_L t)^{\beta}], \tag{3}$$

with static (transversal) and dynamic (longitudinal) relaxation rates λ_T and λ_L, respectively. This function describes correctly the experimental data (see red lines in Fig. 3a). At low T the spectra show nearly no muon-spin relaxation at long times, i.e., very small relaxation rates λ_L. The T-dependence of λ_L is shown in Fig. 3b. With increasing T, λ_L increases and reaches a maximum at $T_g \approx 0.8\,\mathrm{K}$ in agreement with T_g found in $\chi'(T)$. Subsequently, it decays following a T^{-1} behavior up to 10 K after which no dynamic relaxation is observed in agreement with NMR and susceptibility experiments [44]. On the contrary, the static component λ_T increases steeply below T_g [43]. The β value of about 0.5 for $T \geq T_g$ indicates a broad inhomogeneous distribution of fluctuating dynamical relaxation rates. In the ordered phase β increases and flattens at $T \to 0$ indicating that the spin fluctuations become static. We also observed time-field scaling of the muon asymmetry which points to a cooperative mechanism and to the presence of critical spin fluctuations. The overall behavior can not be ascribed to either canonical spin glasses or to other disorder-driven mechanisms. This rather suggests a novel state of matter close to a FM QCP.

In CeFePO we have surely a delicate interplay between FM and AFM correlations which causes strong frustration and might favor exotic states. An interesting idea was proposed by Thomson et al. who suggest a helical glass state [58]. This state is the result of very small disorder and strong FM fluctuations which destabilize the FM state and enhances the susceptibility towards incommensurate, spiral magnetic ordering. Although CeFePO is a stoichiometric compound the best samples have a relatively small resistivity ratio of about 5 which is due to weak disorder but also to the strong FM fluctuations present at low T. In principle, the amount of disorder that is needed to generate the spiral state can be very small, therefore we can not ruled out this mechanism.

2.2 $YbNi_4P_2$

After the discovery of high-temperature superconductivity in the intermetallic pnictides with a quasi 2D structure like RFeAsO (R = rare earth), see Fig. 1, we started to investigate pnictides which crystallize in the quasi-one-dimensional tetragonal $ZrFe_4Si_2$ structure type [59]. Reducing the dimensionality of a magnetic system is one of the routes to lower its transition temperature. Other routes might be having a system with competing interactions or geometrical frustration, or with a pronounced Kondo effect. $YbNi_4P_2$ seems to be one of the rare cases where all these ingredients are present. In fact, the discovery of a ferromagnetic phase transition in a polycrystal of $YbNi_4P_2$ at a record low Curie temperature of $T_C = 0.17\,\mathrm{K}$ [32] for a stoichiometric compound was a surprise and important for the study of FM quantum criticality [34].

The crystalline quasi-1D structure of $YbNi_4P_2$ is shown in inset of the Fig. 4a [32]: It can be seen as isolated chains along the c direction of edge-connected Ni tetrahedra, with adjacent chains linked by Ni-Ni bonds between corners of the tetrahedra with the lattice parameter $a = 7.0565\,\text{Å}$ being almost twice as large as $c = 3.5877\,\text{Å}$. The Yb atoms are located in the channels between these Ni tetrahedral chains. The quasi-1D character of the structure is reflected in the electronic structure of this material. Non-correlated band-structure calculations show that three sheets of the Fermi surface have a pronounced 1D character [32] and this is clearly seen in the large anisotropy of the electrical transport properties, i.e., the resistivity where $\rho_a/\rho_c \approx 5$ at 1.8 K [60].

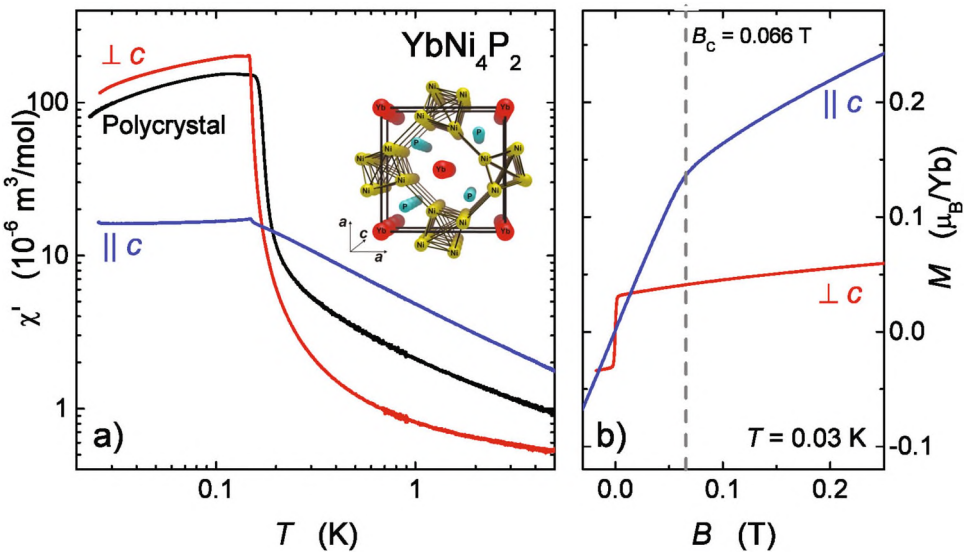

Fig. 4. a) AC susceptibility $\chi'(T)$ of a poly and a single crystal of $YbNi_4P_2$ at $B = 0$. The susceptibility was measured with a modulated magnetic field of about $15\,\mu$T applied parallel (blue curve) and perpendicular (red curve) to the crystallographic c-axis. The Curie temperature of the polycrystal is 0.17 K [32] whereas for the single crystal it is 0.15 K [34]. At about 0.2 K the blue and red curves cross each other indicating that the magnetic moments align along the magnetic hard direction, i.e. within the ab-plane. Inset: a) Stereoscopic view of the tetragonal quasi-1D structure of $YbNi_4P_2$ with the Yb atoms aligned in chains along the c-axis. b) Estimation of the field dependence of the magnetization $M(B)$ for $B \parallel c$ and $\perp c$ obtained by integrating the field dependence of $\chi'(B)$ measured at 0.03 K. The values of the magnetization are in agreement with those found for the polycrystal [32]. Above the critical field $B_c = 0.066$ T the moments are polarized along the c direction.

Measurements of the susceptibility $\chi(T)$ indicated a clear Curie-Weiss behavior between 50 and 400 K with an effective moment $\mu_{eff} = 4.52\,\mu_B$ as expected for magnetic Yb^{3+} ions, thus supporting the absence of a Ni-moment. Adjacent Yb chains are shifted by $c/2$ and the local orthorhombic symmetry at the Yb-site is rotated by 90° from chain to chain, while keeping the symmetry on the Yb site the same. This causes geometrical frustration between neighboring chains that, together with strong correlations, may strongly enhance quantum fluctuations. The orthorhombic CEF splits the $J = 7/2$ energy levels leaving a Kramers doublet as ground state [61] with the c-axis as the magnetic easy axis [60]. This can be clearly seen in the left frame of Fig. 4 where the AC susceptibility $\chi'(T)$ measured with a modulated field $B = 15\,\mu$T parallel and perpendicular to the c-axis is plotted. The susceptibility $\chi'_{\parallel}(T)$ with $B \parallel c$ (blue curve) is larger than that with $B \perp c$, $\chi'_{\perp}(T)$ (red curve), from high temperatures down to about 0.2 K. However, at about 0.2 K $\chi'_{\parallel}(T)$ crosses $\chi'_{\perp}(T)$ and the FM ordering is then in the ab-plane, causing $\chi'_{\perp}$ to diverge sharply just above $T_C = 0.15$ K up to a value of about $200 \times 10^{-6}\,m^3/mol$ ($\chi'_{SI} \approx 4$). At T_C, a pronounced increase of $\chi''_{\perp}(T)$ is observed, representative of energy dissipation [34,56]. This is not the only ferromagnet which shows such an inversion of the magnetic anisotropy at low T. Further examples among Kondo-lattice systems are, e.g., CeRuPO [62], YbNiSn [63] or $Yb(Rh_{0.73}Co_{0.27})_2Si_2$ [64]. In $YbNi_4P_2$ the crossing of susceptibilities can not be explained by a scenario with competing exchange interactions [65], but it needs a more complex approach. $YbNi_4P_2$ is definitely not a classical system and

the physics close to T_C is dominated by strong quantum fluctuations. This can be seen in the behavior of $\chi'_\perp(T)$: For a Ising or Heisenberg classical systems $\chi'_\perp(T)$ would diverge at temperature close to T_C with a power law function with well known universal exponents. $\chi'_\perp(T)$ in Fig. 4 diverges just above T_C with a much stronger function than a power law. This function is stronger than the one expected for a pure 1D-Ising ferromagnet [66]. A new proposal has been put forward by Kruger et al. who take into account strong quantum fluctuations along the magnetic hard axis [67].

Integrating the field dependence of $\chi'(B)$ measured at 0.03 K we could obtain a good approximation for the field dependence of the magnetization $M(B)$ for $B \parallel c$ and $B \perp c$. The values of the magnetization are in agreement with those found for the polycrystal [32]. The magnetization with $B \perp c$ displays a clear jump of about $0.05\,\mu_B$/Yb at $B = 0$ and saturates immediately after that, indicating that the coercive field is very small. On the other hand, the magnetization $B \parallel c$ is zero at $B = 0$ and rises linearly up to a critical field $B_c = 0.66$ T where the moments are polarized along the c direction. These observations point to in-plane FM order with an ordered moment of about $0.05\,\mu_B$/Yb although neutron scattering experiments are needed to determine the exact magnetic structure. This is in agreement with recent zero-field μSR experiments which proved static magnetic order with a strongly reduced ordered Yb^{3+} moment of 0.025 μ_B/Yb [68]. The large reduction of the moment is mainly due to the Kondo effect. In this material a Kondo temperature of 8 K (for the lowest-lying CEF Kramers doublet) was estimated from the entropy extracted from measurements of the specific heat [32].

Despite the very low Curie temperature, $YbNi_4P_2$ shows a series of other interesting properties, namely peculiar non-Fermi liquid behavior in transport and thermodynamic quantities above T_C. The temperature dependence of the resistivity (T) and the Seebeck coefficient $S(T)$ between 2 and 300 K identify $YbNi_4P_2$ as a Kondo lattice with strong interactions between $4f$ and conduction electrons. For instance, $\rho(T)$ decreases linearly down to 50 K and drops rapidly below 20 K, due to the onset of coherent Kondo scattering. At lower temperatures the resistivity is quasi linear-in-T just above T_C and shows a clear kink at T_C. This NFL behavior is commonly taken as evidence for quantum fluctuations associated with a QCP [69] when it is observed over a large T range. In our case, a clean $\Delta\rho \sim T$ behaviour can be observed only in a relatively small temperature window $0.15 \leq T \leq 1$ K, because for $T > 1$ K the effect of the Kondo scattering influences $\rho(T)$.

Specific heat data, shown in Fig. 5a, strongly confirm that $YbNi_4P_2$ is a FM ordered HF system. A sharp, λ-type anomaly is observed at T_C indicating a second-order phase transition with a small entropy change (1% of R$ln2$, with R = 8.31 J/molK). Below T_C a huge Sommerfeld coefficient, $\gamma_0 \approx 2\,\mathrm{J/K^2mol}$ reflects the existence of heavy quasi-particles with an electronic mass two to three orders of magnitude larger than the bare electron mass. Remarkably, at $B = 0$, C/T increases below 6 K, following a $T^{-0.43}$ power law down to 0.2 K, where classical thermal fluctuations associated with the phase transition set in. A similar power law ($C/T \propto T^{-0.4}$) was observed in $YbRh_2Si_2$, a system with strong FM fluctuations in which quantum criticality has been extensively investigated [19]. The large increase of C/T for $T \to T_C$ excludes a Fermi-liquid ground state, because for a Kondo temperature $T_K = 8$ K, C/T should become almost constant below 1 K. Ferromagnetic fluctuations were also observed in NMR experiments with $1/T_1T \propto T^{-3/4}$ in a broad T-range above T_C [70]. This and the distinct NFL properties above T_C are clear indicators that $YbNi_4P_2$ is located in the close vicinity of a FM QCP and this motivated the growth of As substituted single crystals in order to tune T_C to zero.

Three single crystals of the series $YbNi_4(P_{1-x}As_x)_2$ were grown with $x = 0.04$, 0.08, and 0.13. The phase transition was investigated in specific heat, thermal expansion and AC susceptibility [34]. The specific heat of all samples in zero field is shown

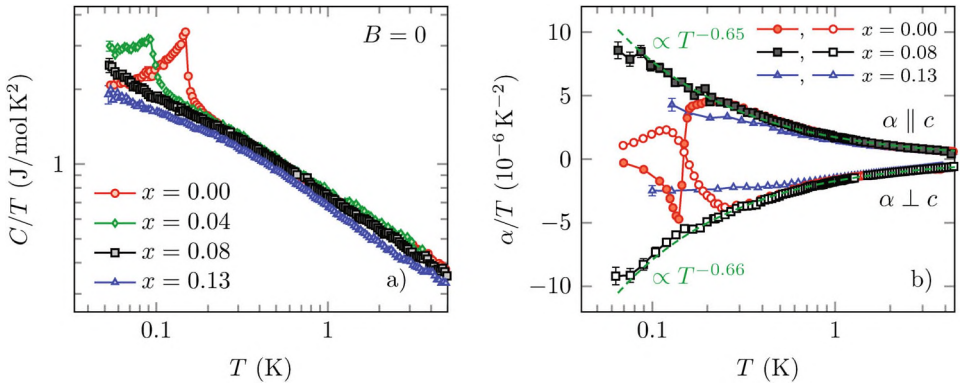

Fig. 5. a) Specific heat $C(T)$ plotted as C/T vs. T of $YbNi_4(P_{1-x}As_x)_2$ with $x = 0$, 0.04, 0.08 and 0.13 at zero magnetic field. The FM transition temperature is tuned to zero with increasing x and for $x = 0.08$ C/T follows a $T^{-0.43}$ power law within the error bars [34]. b) Linear thermal expansion coefficient $\alpha(T)$ plotted as $\alpha(T)/T$ vs. T for the samples with $x = 0$, 0.08 and 0.13 measured in zero field. $\alpha(T)$ measured along the c axis is positive and negative when measured perpendicular to the c-axis. The volume thermal expansion coefficient is therefore negative. While for $YbNi_4P_2$ the change of sign in $\alpha(T)$ indicates the phase transition at T_C, for the $x = 0.08$ sample no inflection can be seen down to 0.06 K. The orange dashed lines emphasise the $T^{-0.65}$ and $T^{-0.66}$ power-law increase of α/T vs. T. For the $x = 0.13$ sample the coefficient $\alpha(T)/T$ saturates below 1 K, indicating non-critical behaviour.

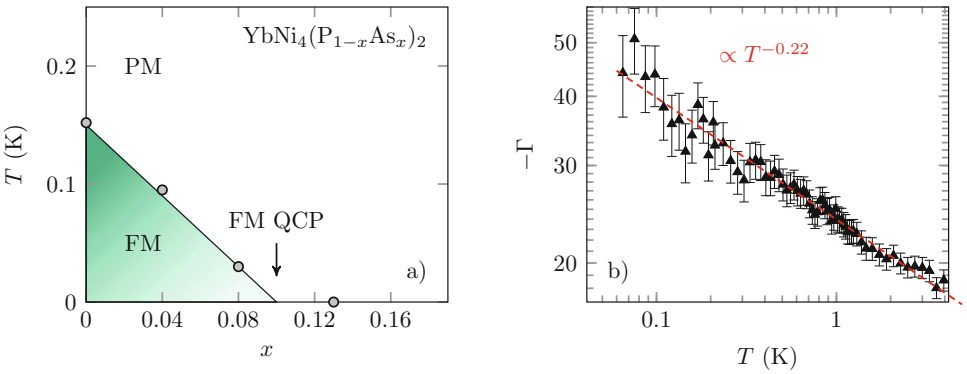

Fig. 6. a) $x-T$ phase diagram of $YbNi_4(P_{1-x}As_x)_2$: the FM QCP is located at $x_c \approx 0.1$. b) T-dependence of the dimensionless thermal Grüneisen ratio $\Gamma(T)$ for $x = 0.08$ whose divergence indicates the presence of quantum critical fluctuations. The dashed red line emphasizes the $T^{-0.22}$ divergence of $\Gamma(T)$ [34].

in Fig. 5a. The phase transition remains second-order in the $x = 0.04$ sample and ferromagnetic. In fact, C/T of the same sample was measured with $B \perp c$ and the transition is shifted to higher T with increasing B. At $x = 0.08$, no phase transition could be detected in C/T down to 0.04 K where C/T increases with the same T-dependence as in $YbNi_4P_2$ (black points in Fig. 5a). However, measurements of $\chi'(T)$ down to 0.02 K picked up a FM transition at 0.028 K. At $x = 0.13$ no phase transition is observed down to 0.02 K and C/T vs. T seems to follow the same power law down to 0.1 K, but with smaller absolute values. The observed NFL features suggest the

presence of strong quantum fluctuations but do not directly imply the existence of a FM QCP, i.e. that these fluctuations become critical at the QCP [35,71].

To provide direct evidence for critical fluctuations we measured the volume thermal expansion coefficient $\beta = \alpha_{\parallel} + 2\alpha_{\perp}$ (with $\alpha_{\parallel}$ and $\alpha_{\perp}$ being the linear expansion coefficients along c and a) in order to extract the Grüneisen ratio $\Gamma(T)$ at x_c (see Sect. 1). $\Gamma(T)$ should diverge at the QCP with $T^{-1/\nu z}$. The thermal expansion of $x = 0$, 0.08, and 0.13 single crystals is shown in Fig. 5b. For $YbNi_4P_2$ a clear phase transition and a change of sign in $\alpha(T)/T$ is visible at T_C. As in the specific heat for $x = 0.08$ no inflection can be seen down to 0.06 K, in agreement with $T_C = 0.028$ K seen in $\chi'(T)$. The coefficients $\alpha_{\parallel}/T$ and $\alpha_{\perp}/T$ diverge with decreasing T with similar exponents, yielding $\beta/T \propto T^{-0.64}$. This cannot be due to thermal fluctuations associated with the FM phase transition, because these would cause a change in slope above T_C, nor can it be due to the development of a Fermi-liquid state where $\beta/T \sim$ const. For $x = 0.13$, $\alpha(T)/T$ levels off below 1 K.

In Fig. 6 we summarise the key evidences for the presence of a FM-QCP in $YbNi_4P_2$. The x vs. T phase diagram is shown in the left frame. The Curie temperature decreases linearly with incrising x ending at a critical point for $x_c \approx 0.1$. The phase transition remains second order and the NFL behavior is similar for all samples at temperatures above T_C in contrast to the general consensus [25]. More importantly, the dimensionless Grüneisen ratio diverges as $\Gamma(T) \propto T^{-0.22}$ (see Fig. 6b). This implies the presence of quantum critical fluctuations at x_c. The exponent indicates $\nu z \approx 5$, which is far from the prediction for 3D or 2D FM fluctuations. However, this value has been directly obtained by fitting the experimental data without any subtraction of non-critical contributions from $C(T)$ and $\alpha(T)$ which are unknown. Our experiments on $YbNi_4(P_{1-x}As_x)_2$ show that this is the first correlated system in which a FM quantum critical point has been directly observed. The combination of unexpected power-law exponents in all thermodynamic quantities, indicating the presence of strong FM critical fluctuations, can not be explained by any known theory of quantum phase transitions and may reflect the 1D character of the electronic structure and of the in-plane FM order in $YbNi_4P_2$and/or the concurrence of the FM instability with a breakdown of the Kondo effect, similar to what was found for the antiferromagnet $YbRh_2Si_2$ [72].

3 Geometrically frustrated systems

Frustrated magnetism arises in situations where not all pairwise magnetic interactions are satisfied simultaneously, as for example antiparallel coupled moments on equilateral triangles. There is an increasing number of insulating magnets, for which spin liquid physics related to strong quantum fluctuations due to geometrical frustration is discussed [73]. On the other hand, for metallic Kondo lattices, strong quantum fluctuations due to geometrical frustration may act as competing mechanism against the Kondo-singlet formation, stabilizing novel so called fractionalized Fermi liquid phases [74,75]. A "global phase diagram" has been proposed with different magnetically ordered and paramagnetic phases, in which the f-electrons are either itinerant or localized [76–81]. In particular the possibility of a Kondo breakdown QCP may be supported by strong quantum fluctuations. For very strong frustration a "fractionalized" Fermi liquid phase has been predicted, in which local f-moments in a spin liquid state are effectively decoupled from the conduction electrons. Despite this growing interest, only few geometrically frustrated Kondo metals have been studied so far [82,83].

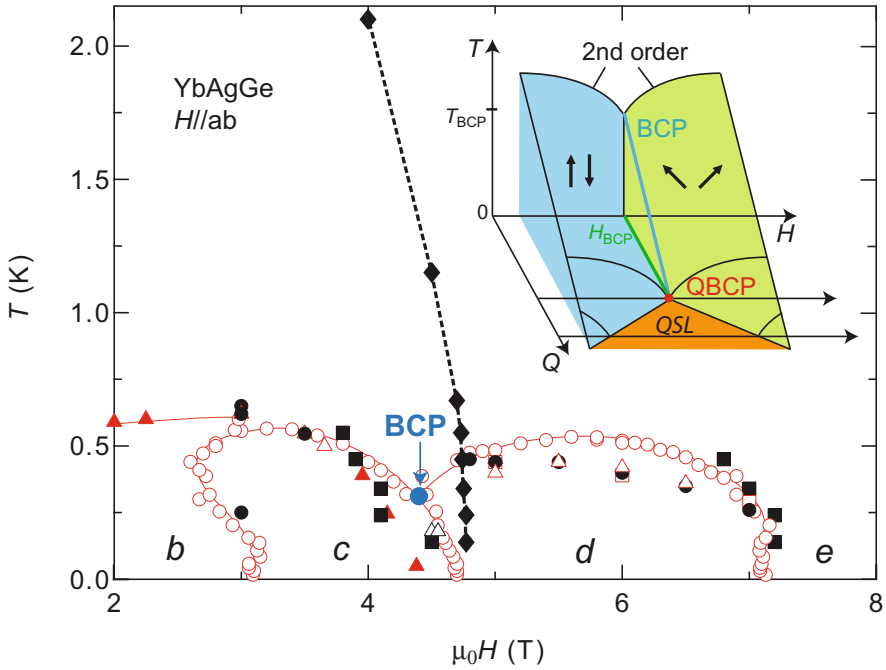

Fig. 7. Low-temperature phase diagram of YbAgGe for magnetic fields applied perpendicular to the hexagonal c-axis. Red points and lines denote phase transitions determined previously [84–86], while black data points indicate phase transitions (circles and squares) zero-crossings (diamonds) in the adiabatic magnetocaloric effect [87]. The blue circle marks the position of a bicritical point at 0.3 K, 4.5 T, where the first-order phase transition line between phases c and d splits into two second order phase lines at elevated temperatures. The inset displays a schematic three-dimensional T-H-Q phase diagram with a line of bicritical points related to a spin-flop that is suppressed to $T = 0$ by increasing quantum fluctuations Q.

3.1 YbAgGe

A particular interesting class of materials is found in the hexagonal ZrNiAl structure where the Zr position could be occupied by the Kondo ions Ce or Yb [88]. The structure consists of two-dimensional distorted Kagome planes stacked along the c-axis with fully frustrated next neighbor interactions. In CePdAl a very peculiar ground state has been found. Here 2/3 of the Ce atoms display a columnar magnetic ordering while 1/3 are remaining paramagnetic as a result of frustration. We have focused our attention on the isostructural Kondo lattice metal YbAgGe. Here, the effect of magnetic frustration is evident from the complex T-H phase diagram at low temperatures, with several commensurate and incommensurate ordered states below 0.6 K [84]. Utilizing an alternating field technique [89], we have recently studied the magnetic Grüneisen ratio or adiabatic magnetocaloric effect $\Gamma_H = T^{-1}(dT/dH)_S$ of YbAgGe for magnetic fields applied along the a-axis, i.e. within the Kagome planes [85]. As shown in Fig. 7, the boundaries of phases c and d are merging near a bicritical point (indicated by the blue arrow). Below $T_{\rm BCP} \approx 0.3$ K a weak hysteresis in magnetostriction [87] signals a first-order transition. Such bi-criticality, as sketched in the inset, for local moment antiferromagnets with weak magnetic anisotropy arises as metamagnetic spin-flop transition. Reducing the ordering temperatures by strong quantum

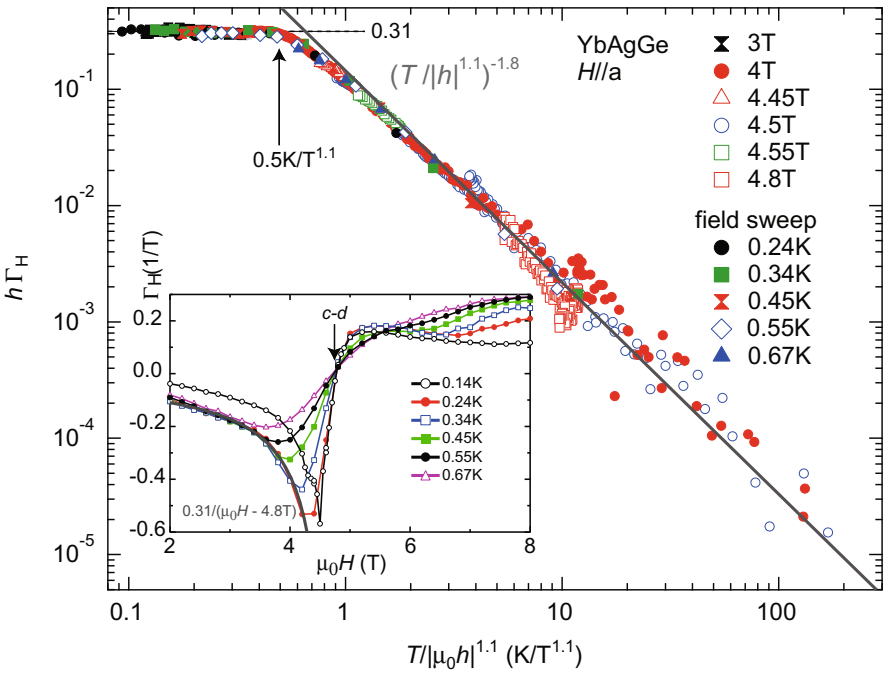

Fig. 8. Quantum critical scaling of the magnetic Grüneisen ratio of YbAgGe as $h\Gamma_H$ vs. $T/|h|^{1.1}$ [87] for $H//a$. Here $h = H - H_{\mathbf{cf}}(T)$. The inset displays Γ_H vs. H for the same field direction. The arrow indicates the zero-crossing of Γ_H, related to the transition between phases c and d.

fluctuations due to geometrical frustration, may result in a quantum bicritical point, beyond which a quantum spin liquid phase opens [87].

The signature of the $c - d$ transition is clearly revealed in measurements of the magnetic Grüneisen ratio, shown in the inset of Fig. 8. The observed zero-crossing of Γ_H indicates an entropy ridge at a critical field $H_{\mathbf{cr}}(T)$ (cf. the black diamonds in Fig. 8). Indeed we observe quantum critical T/h scaling with $h = H - H_{\mathbf{cr}}(T)$ for the magnetic Grüneisen ratio, as shown in Fig. 8 [87]. The scaling behavior is mainly restricted to the T-H regime on the left of the $H_{\mathbf{cr}}(T)$ line. The field dependence of Γ_H is rather anisotropic and diverging behavior in the approach of 4.5 T at low temperatures is only found for the low-field, but not for the high-field side. Such anisotropy is characteristic for quantum bicritical behavior and results from the different natures of the states c and d, separated by this instability. A more detailed analysis of the scaling exponents suggests quasi-one-dimensional fluctuations, which may be promoted by the geometrical frustration in this system [87].

In order to further characterize the field-induced QCP in YbAgGe we have studied the electrical and thermal transport down to 50 mK at various fields applied in the ab-plane [90]. In particular, we have determined the temperature dependence of the normalized Lorenz ratio, $L(T)/L_0$, see Fig. 9. Strikingly the Lorenz ratio near the QCP at 4.5 T is drastically suppressed compared to all other fields for temperatures below 0.1 K. At any magnetic field, the data below about 0.15 K can be fitted by a linear temperature dependence. Extrapolation of this dependence towards $T = 0$ indicates that $L(T)/L_0$ approaches 1, for all fields except the critical field, where it extrapolates to about 0.9 [90]. The data suggest that the Wiedemann-Franz law may be violated near the QCP, similar as recently concluded for $YbRh_2Si_2$ [91].

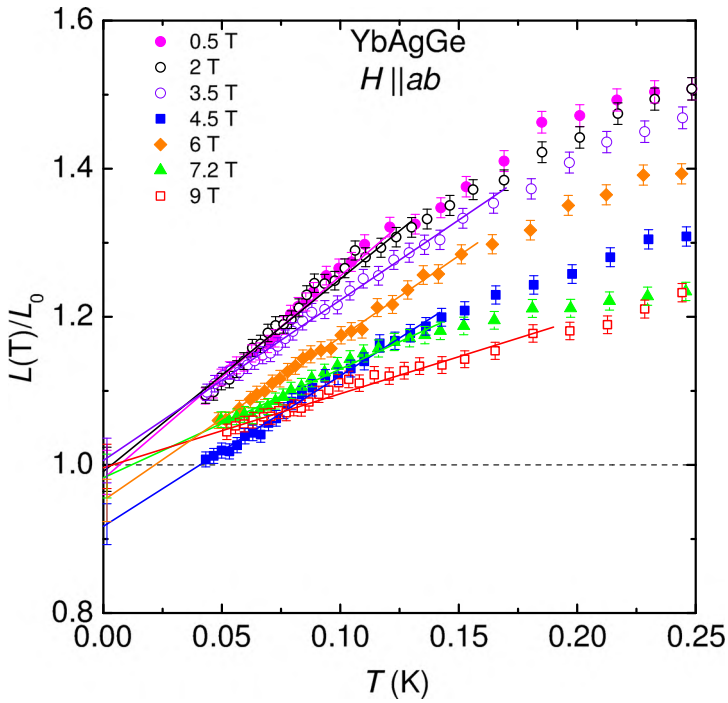

Fig. 9. Temperature dependence of the normalized Lorenz ratio $L(T)/L_0 = \kappa\rho/(L_0 T)$ from thermal conductivity $\kappa(T)$, electrical resistivity $\rho(T)$ measurements ($L_0 = 3\pi^2 k_B^2 e^2$) of YbAgGe for different magnetic fields applied within the ab plane [90]. Error bars near zero temperature indicate systematic error for the extrapolated Lorenz ratio arising from the finite width of the contacts.

3.2 $Pr_2Ir_2O_7$

We now turn to pyrochlore $Pr_2Ir_2O_7$, with local Pr^{3+} magnetic moments and a small concentration of Ir $5d$ conduction electrons [92]. In this system, crystal electric field splitting leads to a magnetic non-Kramers doublet Pr^{3+} state. These moments have a strong local Ising anisotropy and are arranged on the edges of corner-sharing tetrahedra in the pyrochlore structure. Similar as found for prototype spin-ice materials like Dysprosium Titanate [93] strong geometrical frustration arises. In contrast to classical spin ice, we have found that the magnetic entropy clearly drops below the Pauling value upon cooling to below 0.4 K [94], probably related to stronger quantum fluctuations for this effective doublet spin system. Additional complexity arises by the presence of about 10^{-3} Ir conduction electrons per unit cell. Most remarkably, a spontaneous Hall conductivity has been observed below 1.5 K in the absence of magnetic ordering and internal magnetic fields (at least down to about 200 mK where a partial spin freezing has been observed) [95]. We have performed a detailed investigation of the low-temperature specific heat and magnetocaloric effect and found evidence for zero-field quantum criticality in this material [94]. The low-temperature specific heat data (see Fig. 10) suggest unusual low temperature behavior, although the origin of the drastic increase of C/T below 0.4 K is yet unknown. The temperature over magnetic field scaling behavior shown in the right part of Fig. 10 proves that this system is located near a zero-field QCP. The derived scaling exponents do not agree with the predictions for itinerant SDW QCPs, which is not surprising, because of the

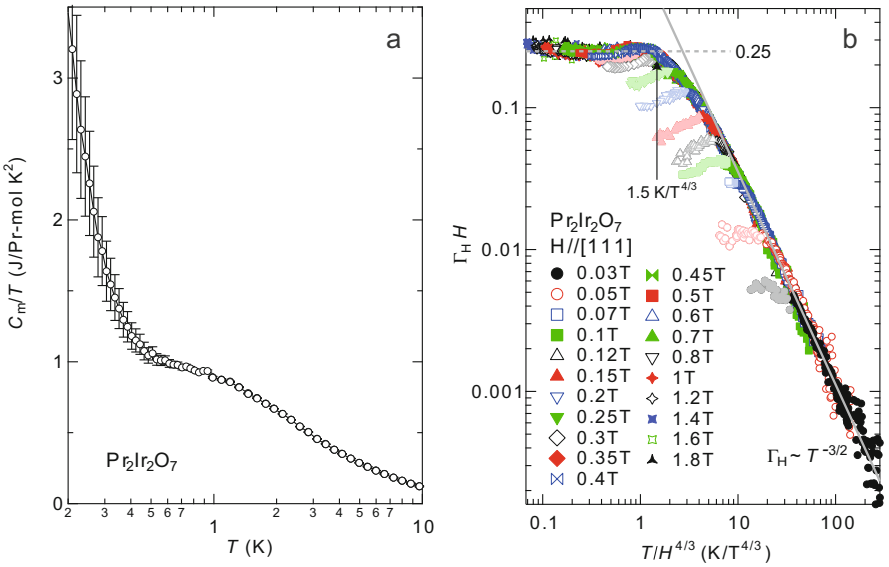

Fig. 10. Low-temperature magnetic specific heat coefficient (a) and quantum critical scaling of the magnetic Grüneisen ratio (b) of pyrochlore $Pr_2Ir_2O_7$ [94].

highly frustrated local Pr^{2+} moments which are at most weakly Kondo screened by the small concentration of charge carriers in this material. Future experiments on the insulating quantum spin-ice material $Pr_2Ir_2O_7$ [96] are planned in order to reveal the importance of charge carriers for quantum criticality in $Pr_2Ir_2O_7$.

4 Quantum criticality hidden by unconventional SC

Various unconventional superconductors like cuprates or iron pnictides display unusual normal state properties, which have been connected to possible QCPs hidden within the SC state. We have focused our attention to the tetragonal $CeCoIn_5$. This heavy-fermion superconductor displays intriguing non-Fermi liquid behavior in the normal state above $T_c = 2.3$ K. In particular the non-Fermi liquid behavior extends to very low temperatures as SC is suppressed close to the upper critical field H_{c2} [20,97,98]. For $H > H_{c2}$ various physical properties have indicated a low-lying FL to NFL crossover. The extrapolation of this crossover in transport or thermodynamic experiments has suggested a field-induced QCP in $CeCoIn_5$, located close or slightly below H_{c2}.

Measurements of the magnetic Grüneisen ratio are best suited to determine the exact location of a field-driven QCP, because $\Gamma_H \sim (H - H_c)^{-1}$ is generally expected, independent of the specific nature of the underlying critical fluctuations [39]. We have implemented an alternating field technique to sensitively probe $\Gamma_H(T, H)$ at different field orientations for $CeCoIn_5$. Despite the anisotropy of the normal state properties of this material, we observe along all different directions $\Gamma_H = 0.85/H$ at $T \to 0$ [99], providing strong evidence for a QCP at zero magnetic field. This universal isotropic divergence is remarkable in view of the strongly anisotropic normal state parameters of the material but fully compatible with the theoretical expectation, which relates the dimensionless prefactor (here 0.85) to universal properties of the QCP. Figure 11 displays T/H scaling behavior of the magnetic Grüneisen parameter. This provides

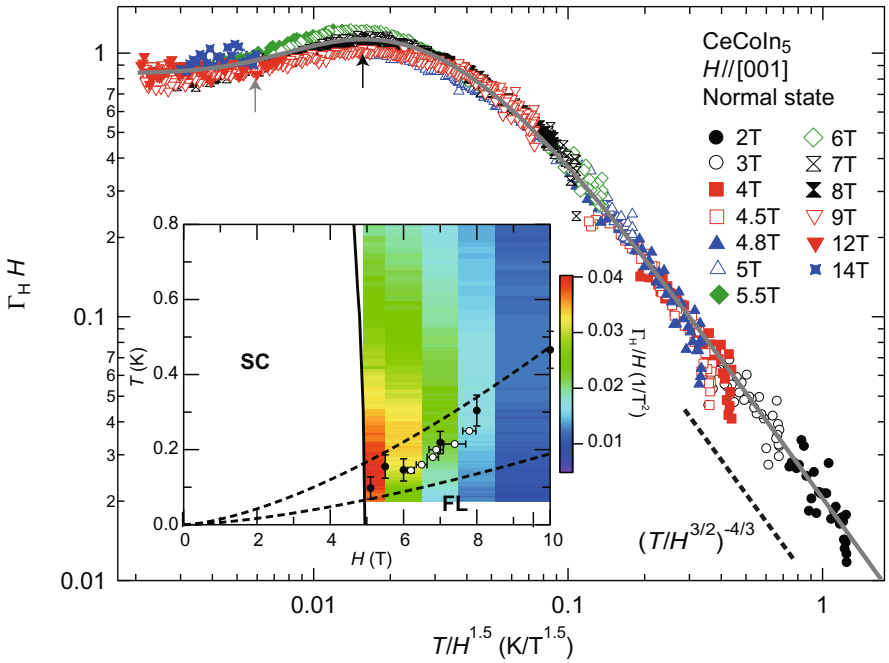

Fig. 11. Magnetic Grüneisen ratio of $CeCoIn_5$ for the field applied along the [001] direction as $\Gamma_H H$ vs. $T/H^{1.5}$ [99]. The phase T-H phase diagram with the boundary of the superconducting (SC) and Fermi liquid (FL) regimes, where the color coding in the normal state represents Γ_H/H is shown in the inset. Open and solid circles represent the onset of FL behavior in Hall effect [97] and thermal expansion [98] measurements, respectively. The two broken lines represent inflection points and maxima of $\Gamma_H H$ (cf. grew and black arrows in Fig. 11), respectively, which are characteristic signatures of the FL to non-Fermi liquid behavior [99].

direct evidence, that without fine-tuning magnetic field (or any other parameter like pressure) the system is already situated right at a QCP. Our results are in contrast to the previous claimed QCP near the upper critical field, derived by linear extrapolation of FL to NFL crossovers in various different properties (cf. circles in Fig. 11). Indeed, the observed scaling behavior of Γ_H indicates, that such linear extrapolation is invalid, and by contrast the FL to NFL crossover has a super-linear dependence (cf. broken lines in Fig. 11), which in fact extrapolates as $T \to 0$ to zero magnetic field.

Our conclusion on zero-field quantum criticality is also supported by measurements within the SC state [99]. As shown in Fig. 12, the low-temperature specific heat shows a very unusual field dependence. For type II superconductors we expect an increase of C/T with H due to the formation of vortex cores. In $CeCoIn_5$, however a decrease of C/T with increasing field is found between 0.1 and 0.7 T. Since C/T in the SC state is determined by the quasiparticle contribution from vortex cores, this is indicates a reduction of the quasiparticle mass upon driving the system away from the zero-field QCP. Relatedly, the magnetic Grüneisen ratio diverges upon reducing the field from 1 T to zero. We have also calculated the field-dependence of the electronic entropy by integration of $\partial S/\partial H = -C\Gamma_H$ [99]. As displayed in Fig. 12, the quasiparticle entropy decreases with increasing field. This is fully consistent with a zero-field QCP, which influences the normal regions in the vortex cores. Thermal conductivity measurements in the SC state have been interpreted in terms of extreme multiband superconductivity, with a tiny critical field of about 10 mT for SC on one

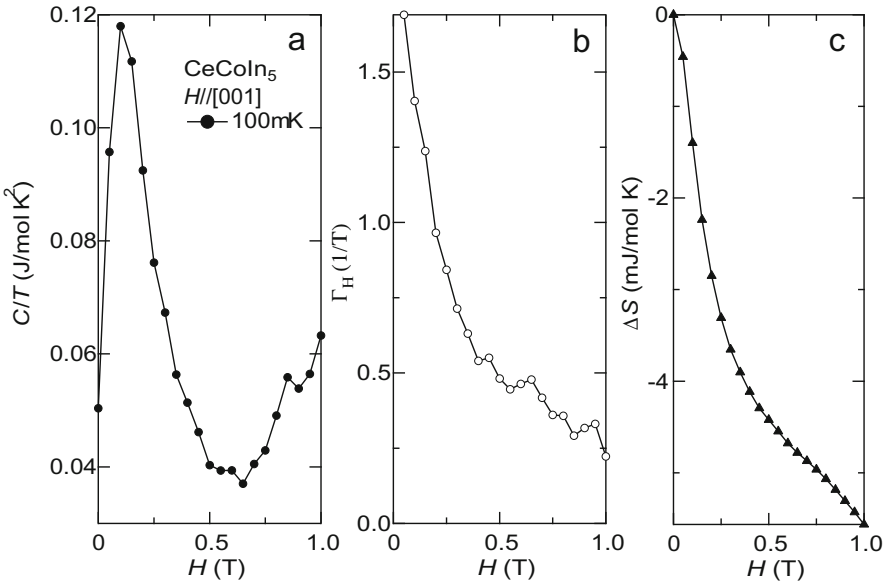

Fig. 12. Field dependence of the electronic specific heat (a), magnetic Grüneisen ratio (b) and entropy (c) of $CeCoIn_5$ at 0.1 K for $H \parallel [001]$ [99].

of the Fermi surfaces [100]. However, such scenario would not explain the above thermodynamic signatures of zero-field quantum criticality, in particular the anomalous field dependence of C/T and the divergence of Γ_H. We also note, that a critical field for quantum criticality near H_{c2} should result in a sign change of $\Gamma_H(H)$ near this field, which is not observed. Therefore, our study disproves the previous proposals and by contrast indicates that $CeCoIn_5$, which has the highest T_c among the family of $Ce_nM_mIn_{3n+2m}$ (M: transition metal) structural variants, is without tuning of any control parameters like field, composition or pressure located directly above a QCP.

5 Summary

The focus of this paper has been to review some recent experiments on QCPs in heavy-fermion metals, with particular emphasis on ferromagnetic and strongly geometrically frustrated materials.

Originally, the search for ferromagnetic quantum critical points was focused on itinerant 3*d*-electron ferromagnets like, e.g., MnSi [26] or $ZrZn_2$ [28], but not on HF systems. This is because the theoretical framework was based on the Stoner theory of itinerant ferromagnetism [6–8] and only a very little number of FM Kondo lattices were known. In the past years the theory on FM criticality was successively extended and improved: It was shown that a FM QCP does not exist in itinerant ferromagnets since these systems are inherently unstable towards a phase transition of first order [21]. This conclusion was indeed confirmed by a growing number of experiments [101]. On the other hand, the number of studies on ferromagnetic HF systems has increased a lot, while the theoretical investigation of FM Kondo lattices has begun only very recently [31]. In this respect, our work makes an important contribution to this field. We have investigated the quantum critical behavior of several FM Kondo lattices and presented in this review two prominent examples: CeFePO and $YbNi_4P_2$. Both systems are metallic, have a Kondo temperature of about 10 K

and a large Sommerfeld coefficient. In addition, they show strong FM fluctuations and NFL behavior at temperatures above their ordering temperatures. Nevertheless, they do not show any transition of the first order. CeFePO displays short-range magnetic ordering with no presence of a FM QCP, while $YbNi_4P_2$ displays FM order at $T_C = 0.15\,\mathrm{K}$ and a FM QCP at a negative chemical pressure. Despite extensive investigations, both states of matter at the FM quantum phase transitions are currently not understood and more work is needed.

Quantum criticality in heavy-fermion metals has long been illustrated by the Doniach diagram, which considers the suppression of magnetic ordering by the Kondo coupling between the f-moments and conduction electrons [4]. More recently, Doniach's diagram was extended: an additional axis, representing magnetic frustration or more precisely the strength of quantum fluctuations, has been introduced [76,77,79–81]. As known from magnetic insulators, strong frustration destabilizes long-range ordering and favors spin-liquid type non-ordered states. The "global phase diagram" combines the physics of strong frustration with that of Kondo interaction in metals. It considers two ways to destabilize magnetic order, i.e. by enhancing the quantum fluctuation with frustration or Kondo screening the moments. Tuning these systems by experimentally accessible control parameters modifies the Kondo interaction and frustration and can induce different types of QCPs [79,102]. In particular it has been argued, that local criticality could emerge in systems with sufficient degree of frustration. Furthermore, a new Fermi liquid phase, in which non-Kondo screened f-moments are forming a spin liquid state, has been predicted theoretically [76]. This "fractionalized Fermi liquid" state has not been experimentally investigated so far. Therefore it is very interesting to experimentally study QCPs in strongly frustrated Kondo metals.

In this paper, we have summarized our experiments on hexagonal YbAgGe [87, 90] and pyrochlore $Pr_2Ir_2O_7$ [94]. The former material is a Kondo lattice where the Yb atoms are located in two-dimensional distorted Kagome planes. The magnetic frustration results in a number of different almost degenerate magnetic phases, that are realized when applying a magnetic field in the ab plane. We have identified a field-induced QCP at 4.5 T by measurements of the magnetic Grüneisen ratio. Interestingly, this instability is caused by a close bi-critical point towards $T = 0$. The scenario is as follows. The strong frustration in this material depresses the nearby ordered states and leads to a quantum bi-critical point, which in contrast to ordinary QCPs has two ordered phases in its vicinity. This causes peculiar scaling behavior in the magnetocaloric effect. Furthermore, in the vicinity of this instability, we have found an anomalous depression of the Lorenz ratio between thermal and electrical conductivity, which suggests (in the $T = 0$ extrapolation) a violation of the Wiedemann-Franz law [90].

For pyrochlore $Pr_2Ir_2O_7$ we have discovered zero-field quantum critical scaling of the magnetic Grüneisen ratio [94]. Previously, a chiral spin liquid state in this "quantum spin-ice" system had been found [95]. Therefore, the new data indicate a new quantum critical spin liquid state. In this system, the charge carrier concentration is likely too low (only about 0.001 per unit cell) to induce Kondo screening. It needs to be studied in future, whether the charge carriers have an influence on the observed thermodynamic signatures of quantum criticality at all.

Finally, we have addressed the heavy-fermion superconductor $CeCoIn_5$ which realizes a QCP inside a SC phase. Both temperature over magnetic field scaling in the normal state as well as the peculiar field dependence of specific heat and the magnetic Grüneisen ratio inside the SC state indicates zero-field quantum criticality [99]. While zero-field quantum criticality in materials like $Pr_2Ir_2O_7$ or $Na_4Ir_3O_8$ [103] may arise due to the strong frustration, it is unclear why a Kondo metal like $CeCoIn_5$ should be situated "accidentally" right at a QCP without fine-tuning of external parameters like pressure, composition or magnetic field. Possibly this is related to the fact

that this material has the highest T_c among the entire family of $Ce_nM_mIn_{3n+2m}$ (M: transition metal) structural variants.

The results reviewed here have been obtained in collaboration with: S. Lausberg, J. Spehling, A. Steppke, A. Jesche, H. Luetkens, A. Amato, C. Baines, C. Krellner and H.-H. Klauss (CeFePO), A. Steppke, R. Küchler, S. Lausberg, E. Lengyel, L. Steinke, R. Borth, T. Lühmann, C. Krellner and M. Nicklas ($YbNi_4P_2$), Y. Tokiwa, J. Dong, M. Garst, S.L. Budko and P.C. Canfield (YbAgGe), Y. Tokiwa, J.J. Ishikawa and S. Nakatsuji ($Pr_2Ir_2O_7$), Y. Tokiwa and E.D. Bauer ($CeCoIn_5$).

This work has been supported within the DFG research unit 960 (Quantum Phase Transitions) by the project "Quantum Critical Point Scenarios in Heavy-Fermion Systems".

References

1. G.R. Stewart, Rev. Mod. Phys. **73**, 797 (2001)
2. H. v. Löhneysen, A. Rosch, M. Vojta P. Wölfle, Rev. Mod. Phys. **79**, 1015 (2007)
3. P. Gegenwart, Q. Si, F. Steglich, Nature Phys. **4**, 186 (2008)
4. S. Doniach, Physica B+C, **91**, 231 (1977)
5. P. Gegenwart, T. Westerkamp, C. Krellner, T. Tokiwa, S. Paschen, C. Geibel, F. Steglich, E. Abrahams, Q. Si, Science **315**, 969 (2007)
6. J. Hertz, Phys. Rev. B **14**, 1165 (1976)
7. A.J. Millis, Phys. Rev. B **48**, 7183 (1993)
8. T. Moriya, *Spin fluctuations in itinerant electron magnetism* (Springer, Berlin, 1985)
9. J. Arndt, O. Stockert, K. Schmalzl, E. Faulhaber, H.S. Jeevan, C. Geibel, W. Schmidt, M. Loewenhaupt, F. Steglich, Phys. Rev. Lett. **106**, 246401 (2011)
10. O. Stockert, J. Arndt, E. Faulhaber, C. Geibel, H.S. Jeevan, S. Kirchner, M. Loewenhaupt, K. Schmalzl, W. Schmidt, Q. Si, F. Steglich, Nature Phys. **7**, 119 (2011)
11. A. Schröder, G. Aeppli, R. Coldea, M. Adams, O. Stockert, H. v. Löhneysen, E. Bucher, R. Ramazashvili, P. Coleman, Nature **407**, 351 (2000)
12. Q. Si, S. Rabello, K. Ingersent, J.L. Smith, Nature **413**, 804 (2001)
13. P. Coleman, C. Pépin, Q. Si, R. Ramazashvili, J. Phys.: Condens. Matter **13**, R723 (2001)
14. T. Senthil, S. Sachdev, M. Vojta, Phys. Rev. B **69**, 035111 (2004)
15. I. Paul, C. Pépin, M.R. Norman, Phys. Rev. Lett. **98**, 026402 (2007)
16. C. Pépin, Phys. Rev. Lett. **98**, 206401 (2007)
17. S. Burdin, D.R. Grempel, A. Georges, Phys. Rev. B **66**, 045111 (2002)
18. M. Vojta, Phys. Rev. B **78**, 125109 (2008)
19. J. Custers, P. Gegenwart, H. Wilhelm, K. Neumaier, Y. Tokiwa, O. Trovarelli, C. Geibel, F. Steglich, C. Pépin, P. Coleman, Nature **424**, 524 (2003)
20. J. Paglione, M.A. Tanatar, D.G. Hawthorn, E. Boaknin, R.W. Hill, F. Ronning, M. Sutherland, L. Taillefer, C. Petrovic, P.C. Canfield, Phys. Rev. Lett. **91**, 246405 (2003)
21. D. Belitz, T.R. Kirkpatrick, T. Vojta, Phys. Rev. Lett. **82**, 4707 (1999)
22. A.V. Chubukov, C. Pépin, J. Rech, Phys. Rev. Lett. **92**, 147003 (2004)
23. G.J. Conduit, A.G. Green, B.D. Simons, Phys. Rev. Lett. **103**, 207201 (2009)
24. U. Karahasanovic, F. Krüger, A.G. Green, Phys. Rev. B **85**, 165111 (2012)
25. T.R. Kirkpatrick, D. Belitz, Phys. Rev. B. **85,** 134451 (2012)
26. C. Pfleiderer, G.J. McMullan, S.R. Julian, G.G. Lonzarich, Phys. Rev. B **55**, 8330 (1997)
27. C. Pfleiderer, S.R. Julian, G.G. Lonzarich, Nature **414**, 427 (2001)
28. M. Uhlarz, C. Pfleiderer, S.M. Hayden, Phys. Rev. Lett. **93**, 256404 (2004)
29. M. Brando, W.J. Duncan, D. Moroni-Klementowicz, C. Albrecht, D. Grüner, R. Ballou, F.M. Grosche, Phys. Rev. Lett. **101**, 026401 (2008)
30. D.A. Sokolov, M.C. Aronson, W. Gannon, Z. Fisk, Phys. Rev. Lett. **96**, 116404 (2006)

31. S. Yamamoto, Q. Si., PNAS **107**, 15704 (2001)
32. C. Krellner, S. Lausberg, A. Steppke, M. Brando, L. Pedrero, H. Pfau, S. Tence, H. Rosner, F. Steglich, C. Geibel, New J. Phys. **13**, 103014 (2011)
33. A. Fernandez-Pañella, D. Braithwaite, B. Salce, G. Lapertot, J. Flouquet, Phys. Rev. B **84**, 134416 (2011)
34. A. Steppke, R. Küchler, S. Lausberg, E. Lengye, L. Steinke, R. Borth, T. Lühmann, C. Krellner, M. Nicklas, C. Geibel, F. Steglich, M. Brando, Science **339**, 933 (2013)
35. T. Westerkamp, M. Deppe, R. Küchler, M. Brando, C. Geibel, P. Gegenwart, A.P. Pikul, F. Steglich, Phys. Rev. Lett. **102**, 206404 (2009)
36. E. Miranda, V. Dobrosavljevi, G. Kotliar, Phys. Rev. Lett. **78**, 290 (1997)
37. A.H. Castro Neto, G. Castilla, B.A. Jones, Phys. Rev. Lett. **81**, 3531 (1998)
38. T. Vojta, J. Phys. A **39**, R143 (2006)
39. L. Zhu, M. Garst, A. Rosch, Q. Si, Phys. Rev. Lett. **91**, 066404 (2003)
40. R. Küchler, N. Oeschler, P. Gegenwart, T. Cichorek, K. Neumaier, O. Tegus, C. Geibel, J.A. Mydosh, F. Steglich, L. Zhu, Q. Si, Phys. Rev. Lett. **91**, 066405 (2003)
41. M. Garst, A. Rosch, Phys. Rev. B **72**, 20 (2005)
42. K.-S. Kim, A. Benlagra, C. Pépin, Phys. Rev. Lett. **101**, 246403 (2008)
43. S. Lausberg, J. Spehling, A. Steppke, A. Jesche, H. Luetkens, A. Amato, C. Baines, C. Krellner, M. Brando, C. Geibel, H.-H. Krauss, F. Steglich, Phys. Rev. Lett. **109**, 216402 (2012)
44. E.M. Brüning, C. Krellner, M. Baenitz, A. Jesche, F. Steglich, C. Geibel, Phys. Rev. Lett. **101**, 117206 (2008)
45. D.A. Zocco, R.E. Baumbach, J.J. Hamlin, M. Janoschek, I.K. Lum, M.A. McGuire, A.S. Sefat, B.C. Sales, R. Jin, D. Mandrus, J.R. Jeffries, S.T. Weir, Y.K. Vohra, M.B. Maple, Phys. Rev. B **83**, 094528 (2011)
46. Y. Luo, Y. Li, S. Jiang, J. Dai, G. Cao, Z. Xu, Phys. Rev. B **81**, 134422 (2010)
47. A. Jesche, Ph.D. thesis, University of Dresden, 2011
48. A. Jesche, T. Förster, J. Spehling, M. Nicklas, M. de Souza, R. Gumeniuk, H. Luetkens, T. Goltz, C. Krellner, M. Lang, J. Sichelschmidt, H.-H. Klauss, C. Geibel, Phys. Rev. B **86**, 020501 (2012)
49. C. de la Cruz, W.Z. Hu, S. Li, Q. Huang, J.W. Lynn, M.A. Green, G.F. Chen, N.L. Wang, H.A. Mook, Q. Si, P. Dai, Phys. Rev. Lett. **104**, 017204 (2010)
50. K. Mydeen, E. Lengyel, A. Jesche, C. Geibel, M. Nicklas, Phys. Rev. B **86**, 134523 (2012)
51. M.G. Holder, A. Jesche, P. Lombardo, R. Hayn, D.V. Vyalikh, S. Danzenbächer, K. Kummer, C. Krellner, C. Geibel, Y. Kucherenko, T.K. Kim, R. Follath, S.L. Molodtsov, C. Laubschat, Phys. Rev. Lett. **104**, 096402 (2010)
52. C. Krellner, Ph.D. thesis, University of Dresden, 2009
53. S. Kitagawa, H. Ikeda, Y. Nakai, T. Hattori, K. Ishida, Y. Kamihara, M. Hirano, H. Hosono, Phys. Rev. Lett. **107**, 277002 (2011)
54. A. Jesche, C. Krellner (to be published)
55. D. Moroni-Klementowicz, M. Brando, C. Albrecht, W.J. Duncan, F.M. Grosche, D. Grüner, G. Kreiner, Phys. Rev. B **79**, 224410 (2009)
56. S. Lausberg, Ph.D. thesis, University of Dresden, 2013
57. J.A. Mydosh, *Spin glasses: An experimental introduction* (Taylor & Francis, London, 1993)
58. S.J. Thomson, F. Krüger, A.G. Green, Phys. Rev. B **87**, 224203 (2013)
59. S. Deputier, O. Pena, T. Le Bihan, J.Y. Pivan, R. Guerin, Physica B **233**, 26 (1997)
60. C. Krellner, C. Geibel, J. Phys.: Conf. Ser. **391**, 012032 (2012)
61. Z. Huesges, O. Stockert, M.M. Koza, C. Krellner, C. Geibel, F. Steglich, Physica Status Solidi (b) **250**, 522 (2013)
62. C. Krellner, N.S. Kini, E.M. Brüning, K. Koch, H. Rosner, M. Nicklas, M. Baenitz, C. Geibel Phys. Rev. B **76**, 104418 (2007)

63. P. Bonville, P. Bellot, J.A. Hodges, P. Imbert, G. Jéhanno, G. Le Bras, J. Hammann, L. Leylekian, G. Chevrier, P. Thuéry, L. D'Onofrio, A. Hamzic, A. Barthélémy, Physica B: Condensed Matter **182**, 105 (1992)
64. S. Lausberg, A. Hannaske, A. Steppke, L. Steinke, T. Gruner, L. Pedrero, C. Krellner, C. Klingner, M. Brando, C. Geibel, F. Steglich, Phys. Rev. Lett. **110**, 256402 (2013)
65. E.C. Andrade, M. Brando, C. Geibel, M. Vojta, Phys. Rev. B **90**, 075138 (2014)
66. E. Ising, Z. Phys. A **31**, 253 (1925)
67. F. Krüger, F., C.J. Pedder, A.G. Green, Phys. Rev. Lett. **113**, 147001 (2014)
68. J. Spehling, M. Günther, C. Krellner, N. Yéche, H. Luetkens, C. Baines, C. Geibel, H.-H. Klauss, Phys. Rev. B **85**, 140406 (2012)
69. F.M. Grosche, S.R. Julian, N.D. Mathur, F.V. Carter, G.G. Lonzarich, Physica B **237**, 197 (1997)
70. R. Sarkar, P. Khuntia, C. Krellner, C. Geibel, F. Steglich, M. Baenitz, Phys. Rev. B **85**, 140409 (2012)
71. C. Pfleiderer, P. Böni, T. Keller, U.K. Rößler, A. Rosch, Science **316**, 1871 (2007)
72. S. Paschen, T. Lühmann, S. Wirth, P. Gegenwart, O. Trovarelli, C. Geibel, F. Steglich, P. Coleman, Q. Si, Nature **432**, 881 (2004)
73. Balents, L. Nature **464**, 199 (2010) and references therein
74. S. Burdin, D.R. Grempel, A. Georges, Phys. Rev. B **66** (2002)
75. T. Senthil, M. Vojta, S. Sachdev, Phys. Rev. B **69**, 035111 (2004)
76. M. Vojta, Phys. Rev. B **78**, 125109 (2008)
77. Q. Si, Physica B **378-380**, 23 (2006)
78. S. Friedemann, T. Westerkamp, M. Brando, N. Oeschler, S. Wirth, P. Gegenwart, C. Krellner, C. Geibel, F. Steglich, Nature Phys. **5**, 465 (2009)
79. Q. Si, Phys. Status Solidi B **247**, 476 (2010)
80. P. Coleman, A. Nevidomskyy, J. Low Temp. Phys. **161**, 182 (2010)
81. J. Custers, P. Gegenwart, C. Geibel, F. Steglich, P. Coleman, S. Paschen, Phys. Rev. Lett. **104**, 186402 (2010)
82. M.S. Kim, M.C. Aronson, Phys. Rev. Lett. **110**, 017201 (2013)
83. V. Fritsch, N. Bagrets, G. Goll, W. Kittler, M.J. Wolf, K. Grube, C.-L. Huang, H. v. Löhneysen, Phys. Rev. B **89**, 054416 (2014)
84. G.M. Schmiedeshoff, E.D. Mun, A.W. Lounsbury, S.J. Tracy, E.C. Palm, S.T. Hannahs, J.-H. Park, T.P. Murphy, S.L. Budko, P.C. Canfield, Phys. Rev. B **83**, 180408 (2011)
85. Y. Tokiwa, A. Pikul, P. Gegenwart, F. Steglich, S.L. Budko, P.C. Canfield, Phys. Rev. B **73**, 094435 (2006)
86. E. Mun, S.L. Budko, P.C. Canfield, Phys. Rev. B **82**, 174403 (2010)
87. Y. Tokiwa, M. Garst, P. Gegenwart, S.L. Budḱo, P.C. Canfield, Phys. Rev. Lett. **111**, 116401 (2013)
88. R. Pottgen, B. Gibson, R.K. Kremer, Z. Kristallogr. - New Cryst. Struct. **212**, 58 (1997)
89. Y. Tokiwa, P. Gegenwart, Rev. Sci. Instr. **82**, 013905 (2011)
90. J.K. Dong, Y. Tokiwa, S.L. Bud'ko, P.C. Canfield, P. Gegenwart, Phys. Rev. Lett. **110**, 176402 (2013)
91. H. Pfau, S. Hartmann, U. Stockert, P. Sun, S. Lausberg, M. Brando, S. Friedemann, C. Krellner, C. Geibel, S. Wirth, S. Kirchner, E. Abrahams, Q. Si, F. Steglich, Nature **484**, 493 (2012)
92. S. Nakatsuji, Y. Machida, Y. Maeno, T. Tayama, T. Sakakibara, J. van Duijn, L. Balicas, J.N. Millican, R.T. Macaluso, J.Y. Chan, Phys. Rev. Lett. **96**, 087204 (2006)
93. D.J.P. Morris, D.A. Tennant, S.A. Grigera, B. Klemke, C. Castelnovo, R. Moessner, C. Czternasty, M. Meissner, K.C. Rule, J.-U. Hoffmann, K. Kiefer, S. Gerischer, D. Slobinsky, R.S. Perry, Science **326**, 411 (2009)
94. Y. Tokiwa, J.J. Ishikawa, S. Nakatsuji, P. Gegenwart, Nature Mat. **13**, 356 (2014)
95. Y. Machida, S. Nakatsuji, S. Onoda, T. Tayama, T. Sakakibara, Nature **463**, 210 (2010)
96. K. Kimura, S. Nakatsuji, J.-J. Wen, C. Broholm, M.B. Stone, E. Nishibori, H. Sawa, Nature Comm. **4**, 1934 (2013)

97. S. Singh, C. Capan, M. Nicklas, M. Rams, A. Gladun, H. Lee, J.F. DiTusa, Z. Fisk, F. Steglich, S. Wirth, Phys. Rev. Lett. **98**, 057001 (2007)
98. S. Zaum, K. Grube, R. Schäfer, E.D. Bauer, J.D. Thompson, H.V. Löhneysen, Phys. Rev. Lett. **106**, 087003 (2011)
99. Y. Tokiwa, E.D. Bauer, P. Gegenwart, Phys. Rev. Lett. **111**, 107003 (2013)
100. G. Seyfarth, J.P. Brison, G. Knebel, D. Aoki, G. Lapertot, J. Flouquet, Phys. Rev. Lett. **101**, 046401 (2008)
101. M. Brando, et al., Rev. Mod. Phys. (unpublished)
102. J. Custers, K-A. Lorenzer, M. Müller, A. Prokofiev, A. Sidorenko, H. Winkler, A.M. Strydom, Y. Shimura, T. Sakakibara, R. Yu, Q. Si, S. Paschen, Nat. Mater. **11**, 189 (2012)
103. Y. Singh, Y. Tokiwa, J. Dong, P. Gegenwart, Phys. Rev. B **88**, 220413(R) (2013)